Scalar models for the generalized Chaplygin gas and the structure formation constraints

Júlio C. Fabris[1] and Thaisa C.C. Guio[1]

[1] *Universidade Federal do Espírito Santo, Departamento de Física*

Av. Fernando Ferrari, 514, Campus de Goiabeiras,

CEP 29075-910, Vitória, Espírito Santo, Brazil

(Dated: November 2, 2010)

Abstract

The generalized Chaplygin gas model represents a tentative to unify dark matter and dark energy. It is characterized by a fluid with an equation of state $p = -A/\rho^{\alpha}$. It can be obtained from a generalization of the DBI action for a scalar, tachyonic field. At background level, this model gives very good results, but it suffers from many drawbacks at perturbative level. We show that, while for background analysis it is possible to consider any value for α, the perturbative analysis must be restricted to positive values of α. This restriction can be circumvented if the origin of the generalized Chaplygin gas is traced back to a self-interacting scalar field, instead of the DBI action. But, in doing so, the predictions coming from formation of large scale structures reduce the generalized Chaplygin gas model to a kind of quintessence model, and the unification scenario is lost. However, if the unification condition is imposed from the beginning as a prior, the model may remain competitive.

PACS numbers: 98.80.Cq, 98.80.-k, 98.80.Bp

I. INTRODUCTION

A lot of effort has been devoted in the last decades to determine the matter-energy content of the universe. This effort concentrates not only on the determination of the amount of the different components of the cosmic budget, but also on identifying their nature. The different components predicted by the standard model of elementary particles (baryons, radiation and neutrinos) are believed to be known with high precision. Expressed in terms of the ratio to the density necessary to have a flat spatial section (the critical density), the recent estimations lead to a baryonic parameter density today given by $\Omega_{b0} = 0.0456 \pm 0.0016$, while the radiation density is given by $\Omega_{\gamma 0} \sim 5 \times 10^{-5}$ [1]. The neutrino density depends on the number of neutrino species and their masses, but estimations lead to values close to that found for radiation. Summing up all these contributions, the so-called ordinary matter (including under this concept radiation and neutrinos) give a very low mass compared with the critical mass. However, the general features of the spectrum of anisotropies in cosmic microwave background radiation imply that the total matter density of the universe must be very close to the critical one. In the reference [1], using 7-years WMAP measurements, Baryonic Accoustic Oscillations (BA0) and Supernova type Ia (SN Ia) data, the curvature parameter is found to be $\Omega_{k0} = -0.0057^{+0.0067}_{-0.0068}$: the spatial section of the universe is essentially flat, and the total density of mass/energy existing in the universe must be very close to the critical value. Hence, most of the matter/energy of the universe comes from the contributions not predicted by the standard model of elementary particles.

The dynamics of galaxies and clusters of galaxies presents important anomalies, requiring the presence of a pressureless, non-baryonic component, dubbed dark matter, to be explained. The anisotropy spectrum of CMB and the present stage of accelerated universe require the presence of another fluid, in principle exhibiting negative pressure, dubbed dark energy. For a recent review of these evidences, see reference [2]. The main quoted candidates to be the constituents of dark matter are axions and neutralinos [3], but these candidates come from fundamental physical theories not yet tested experimentally. For dark energy, the most natural candidate is the cosmological constant [4]. An important

alternative to the cosmological constant as the dark energy component is a dynamical scalar field called quintessence [5]. All these proposals to the dark sector of the universe have their advantages and their drawbacks, that are exposed in the quoted references.

A quite different alternative to describe the dark sector of the universe is the so-called unified scenario where both components are represented by a unique one playing at same time the rôles of dark matter and dark enegy. The prototype of the unification scenario is the Chaplygin gas (CG) model [6–10] which, in its generalized form, reads

$$p = -\frac{A}{\rho^{\alpha}}. \tag{1}$$

When $\alpha = 1$ we recover the original Chaplygin gas model, which has an interesting connection with the Nambu-Goto action [10]. Using the Friedmann-Lemaître-Robertson-Walker metric and inserting the equation of state (1) into the conservation law for a fluid

$$\dot{\rho} + 3\frac{\dot{a}}{a}(\rho + p) = 0, \tag{2}$$

we can express ρ as function of the scale factor a:

$$\rho = \left\{ A + \frac{B}{a^{3(1+\alpha)}} \right\}^{\frac{1}{1+\alpha}}, \tag{3}$$

indicating that the GCG behaves as pressureless matter for $a \to 0$ and as a cosmological constant when $a \to \infty$. This is the main idea of the unification program.

The Generalized Chaplygin Gas (GCG) model has been tested against many different observational data, like Supernova type Ia(SN Ia) [11], Cosmic Microwave Background Radiation (CMB) [12–14], matter power spectrum (PS) [15, 16]. The general scenario emerging from these different tests is not uniform, depending on the priors and on the statistics scheme. Initially, it has been argued that the CMB tests [12, 13] favor a scenario around $\alpha = 0$, which essentilly reduces the GCG model to the ΛCDM model. But, in reference [14], by using the integrated Sachs-Wolfe effect, models with $\alpha \sim 300$ seem also to be favored. On the other hand, SN Ia tests favor negative values of α [11]. The perturbative analysis for negative values of α is not allowed due to resulting negative values of the squared sound velocity [16].

We intend to address in the present work the last feature of the GCG model. Is it possible to consider negative values of α using a perturbative analysis? Negative squared sound velocity appears, for $\alpha < 0$, in the fluid representation of the GCG model. The original, more fundamental, representation of the GCG model, is given by the DBI action [7, 10], which employs a scalar, tachyonic field. In reference [17] it has been shown that, for $\alpha = 1$ (original Chaplygin gas model) the DBI action gives the same perturbative expressions as those found in the fluid representation, but that such equivalence, at perturbative level, is broken if a self-interacting scalar field is used to represent the CG model instead of the DBI action.

In the present work, we extend the analysis to the case of the GCG model. It will be shown that the complete equivalence of the DBI action and the fluid representation remains for $\alpha \neq 1$. A self-interacting scalar model for the GCG model will be developped, and in this case, the equivalence is lost at perturbative level. Hence the perturbative analysis can be made even for $\alpha < 0$. The comparison with the observational data will show, however, that positive values of α will be favored, except perhaps when the unification scenario is imposed from the beginning. All analysis will be made at perturbative level, since the background is the same as in the fluid or DBI representations.

In the next section, we show the equivalence of the fluid representation with the DBI representation for the GCG model at the background level. The equivalence is extend to the perturbative level in section III. An equivalent scalar model is developped in section IV, and the perturbative analyis is performed in section V. In section VI we present our conclusions.

II. THE DBI FORMULATION

The DBI action is given by the following expression:

$$L = \sqrt{-g}V(T)\sqrt{1 - T_{;\rho}T^{;\rho}}, \tag{4}$$

where T is a scalar (tachyonic) field, and $V(T)$ is the potential for this field. An energy momentum tensor can be constructed from this action. Variation with respect to the

metric leads to following expression for the energy-momentum tensor:

$$T_{\mu\nu} = \frac{V(T)\partial_\mu T\partial_\nu T}{\sqrt{1 - T_{;\rho}T^{;\rho}}} + V(T)\sqrt{1 - T_{,\rho}T^{;\rho}}g_{\mu\nu}. \tag{5}$$

Comparing with the energy-momentum tensor of a perfect fluid,

$$T_{\mu\nu} = (\rho + p)u_\mu u_\nu - pg_{\mu\nu}, \tag{6}$$

and using the homogeneous, isotropic FLRW metric

$$ds^2 = dt^2 - a(t)^2\gamma_{ij}dx^i dx^j, \tag{7}$$

we obtain the following expressions for the density and pressure:

$$\rho_T = \frac{V(T)}{\sqrt{1 - \dot{T}^2}}, \quad p_T = -V(T)\sqrt{1 - \dot{T}^2}. \tag{8}$$

This leads to the equation of state

$$p_T = -\frac{V(T)^2}{\rho_T}. \tag{9}$$

For $V(T) = \sqrt{A} =$ constant, the equation of state (9) represents the traditional Chaplygin gas model.

The GCG, characterized by the equation of state

$$p = -\frac{A}{\rho^\alpha}, \tag{10}$$

can be obtained from the action

$$L_T = \sqrt{-g}V(T)\left[1 - (\partial_\rho T\partial^\rho T)^{\frac{1+\alpha}{2\alpha}}\right]^{\frac{\alpha}{1+\alpha}}, \tag{11}$$

where $V(T) = A^{\frac{1}{1+\alpha}} =$ constant. In fact, from (11), we have the energy-momentum tensor

$$T_{\mu\nu} = \frac{V(T)(\partial_\rho T\partial^\rho T)^{\frac{1-\alpha}{2\alpha}}\partial_\mu T\partial_\nu T}{\left[1 - (\partial_\rho T\partial^\rho T)^{\frac{1+\alpha}{2\alpha}}\right]^{\frac{1}{1+\alpha}}} + V(T)\left[1 - (\partial_\rho T\partial^\rho T)^{\frac{1+\alpha}{2\alpha}}\right]^{\frac{\alpha}{1+\alpha}}g_{\mu\nu}. \tag{12}$$

A direct comparison with the perfect fluid energy-momentum tensor (6), leads to

$$\rho_T = \frac{V(T)}{\left[1-(\partial_\rho T\partial^\rho T)^{\frac{1+\alpha}{2\alpha}}\right]^{\frac{1}{1+\alpha}}}, \tag{13}$$

$$p_T = -V(T)\left[1-(\partial_\rho T\partial^\rho T)^{\frac{1+\alpha}{2\alpha}}\right]^{\frac{\alpha}{1+\alpha}}, \tag{14}$$

$$u_\mu = \frac{\partial_\mu T}{\sqrt{\partial_\rho T\partial^\rho T}}. \tag{15}$$

III. PERTURBATIONS OF THE GENERALIZED DBI ACTION

The perturbation of the perfect fluid energy-momentum tensor (6) is now carried out using the synchronous coordinate condition $h_{\mu 0}=0$. The components of the perturbed energy-momentum tensor are

$$\delta T_{00} = \delta\rho, \tag{16}$$

$$\delta T_{0i} = (\rho+p)\delta u_i, \tag{17}$$

$$\delta T_{ij} = -ph_{ij}-\delta p g_{ij}. \tag{18}$$

The perturbation of the generalized DBI action (11) leads, on the other hand, to the following expressions:

$$\delta T_{00} = \frac{1}{\alpha}\frac{V(T)\dot{T}^{\frac{1}{\alpha}}\delta\dot{T}}{\left[1-\dot{T}^{\frac{1+\alpha}{\alpha}}\right]^{\frac{2+\alpha}{1+\alpha}}}, \tag{19}$$

$$\delta T_{0i} = \frac{V(T)\dot{T}^{\frac{1}{\alpha}}\delta\dot{T}}{\left[1-\dot{T}^{\frac{1+\alpha}{\alpha}}\right]^{\frac{1}{1+\alpha}}}, \tag{20}$$

$$\delta T_{ij} = -\frac{V(T)\dot{T}^{\frac{1}{\alpha}}\delta\dot{T}}{\left[1-\dot{T}^{\frac{1+\alpha}{\alpha}}\right]^{\frac{1}{1+\alpha}}}g_{ij}+V(T)\left[1-\dot{T}^{\frac{1+\alpha}{\alpha}}\right]^{\frac{\alpha}{1+\alpha}}h_{ij}. \tag{21}$$

From the general form of the density, pressure and velocity obtained from the energy-momentum tensor of the DBI action, (13,14,15), we obtain, in the synchronous coordinate

condition,

$$\delta\rho_T = \frac{1}{\alpha}\frac{V(T)\dot{T}^{\frac{1}{\alpha}}\delta\dot{T}}{\left[1-\dot{T}^{\frac{1+\alpha}{\alpha}}\right]^{\frac{2+\alpha}{1+\alpha}}}, \tag{22}$$

$$\delta p_T = \frac{V(T)\dot{T}^{\frac{1}{\alpha}}\delta\dot{T}}{\left[1-\dot{T}^{\frac{1+\alpha}{\alpha}}\right]^{\frac{1}{1+\alpha}}}, \tag{23}$$

$$\delta u_i = \frac{\delta T_{,i}}{\dot{T}}. \tag{24}$$

Inserting the expressions (22,23,24) into (19,20,21), we obtain (16,17,18). Hence, the perturbation of the generalized DBI energy-momentum tensor is perfectly equivalent to its fluid counterpart. In this sense, α negative implies a negative squared sound velocity. This can be verified taking the ratio between (23) and (22). In this sense, the extension of the perturbative analysis for negative values of α is forbidden, in opposition to what happens with the background tests, like SNIa or BAO, where the problems connected with the sound velocity do not appear.

IV. SCALAR MODEL

In order to exploit the possibility of $\alpha < 0$ we must abandon the DBI framework. The most general framework besides the DBI is the self-interacting scalar field. This possibility has been touched in [17], but fixing $\alpha = 1$. But, at least for this case, it has been found that neither the unification scenario [11] nor the anti-unification scenario [16] have been resulted from this self-interacting scalar field approach: the matter density parameter was in fact very close to that predicted by the ΛCDM or the quintessential model. The aim of the present investigation is to verify the predictions when all possible values of α are considered.

The action is now given by

$$L = \frac{1}{16\pi G}\sqrt{-g}\left[R - \phi_{;\rho}\phi^{;\rho} + 2V(\phi)\right] + L_m, \tag{25}$$

where $V(\phi)$ defines the potential and L_m is the matter Lagrangian. The field equations

are

$$R_{\mu\nu} - \frac{1}{2}g_{\mu\nu}R = 8\pi G T_{\mu\nu} + \phi_{;\mu}\phi_{;\nu} - \frac{1}{2}g_{\mu\nu}\phi_{;\rho}\phi^{;\rho} + g_{\mu\nu}V(\phi), \tag{26}$$

$$T^{\mu\nu}{}_{;\mu} = 0, \tag{27}$$

$$\Box\phi = -V_{\phi}, \tag{28}$$

where the subscript ϕ indicates derivative with respect to the scalar field.

The equations of motion are

$$3\left(\frac{\dot{a}}{a}\right)^2 = 8\pi G\rho_{\phi} = \frac{\dot{\phi}^2}{2} + V(\phi), \tag{29}$$

$$2\frac{\ddot{a}}{a} + \left(\frac{\dot{a}}{a}\right)^2 = -8\pi G p_{\phi} = -\frac{\dot{\phi}^2}{2} + V(\phi). \tag{30}$$

In the generalized Chaplygin gas model, the energy density behaves as

$$\rho_c = \rho_{c0} g(a)^{\frac{1}{1+\alpha}}, \quad g(a) = \bar{A} + \frac{(1-\bar{A})}{a^{3(1+\alpha)}}. \tag{31}$$

This expression may be rewritten as

$$\Omega_c = \Omega_{c0} g(a)^{\frac{1}{1+\alpha}}, \quad \Omega_c = \frac{8\pi G\rho_c}{3H_0^2}, \quad \Omega_{c0} = \frac{8\pi G\rho_{c0}}{3H_0^2}. \tag{32}$$

Making the substitution

$$tH_0^2 \to t, \quad \frac{V(\phi)}{H_0^2} \to V(\phi), \tag{33}$$

we may write

$$\rho_{\phi} = \frac{\dot{\phi}^2}{2} + V(\phi) = 3\Omega_{c0} g^{\frac{1}{1+\alpha}}, \tag{34}$$

$$p_{\phi} = \frac{\dot{\phi}^2}{2} - V(\phi) = -3\Omega_{c0}\bar{A} g^{-\frac{\alpha}{1+\alpha}}. \tag{35}$$

Hence, we obtain

$$\dot{\phi} = \sqrt{3\Omega_{c0}}\left\{ g^{\frac{1}{1+\alpha}} - \bar{A} g^{-\frac{\alpha}{1+\alpha}} \right\}^{1/2}, \tag{36}$$

$$V(\phi) = \frac{3\Omega_{c0}}{2}\left\{ g^{\frac{1}{1+\alpha}} + \bar{A} g^{-\frac{\alpha}{1+\alpha}} \right\}. \tag{37}$$

This scalar field model reproduces exactly the background of the generalized Chaplygin gas in presence of baryonic matter. When baryons are absent, we find the potential of reference [7].

V. PERTURBATIVE ANALYSIS OF THE SCALAR MODEL

In order to perform a perturbative study of this model, we rewrite the Einstein's equations in the following form:

$$R_{\mu\nu} = 8\pi G\left(T_{\mu\nu} - \frac{1}{2}g_{\mu\nu}T\right) + \phi_{;\mu}\phi_{;\nu} - g_{\mu\nu}V(\phi), \tag{38}$$

$$\Box\phi = -V_{\phi}(\phi), \tag{39}$$

$$T^{\mu\nu}{}_{;\mu} = 0. \tag{40}$$

We choose to employ the synchronous coordinate condition $h_{\mu 0} = 0$ in carrying out the perturbative study. Since all relevant modes are well inside the cosmological horizon, the final results do not depend on this choice.

The standard perturbative calculation using the synchronous coordinate condition, lead to the final set of equations:

$$\ddot{\delta} + 2\frac{\dot{a}}{a}\dot{\delta} - \frac{3}{2}\Omega_m\delta = 2\dot{\phi}\dot{\lambda} - 2V_{\phi}\lambda, \tag{41}$$

$$\ddot{\lambda} + 3\frac{\dot{a}}{a}\dot{\lambda} + \left[\frac{k^2}{a^2} + V_{\phi\phi}\right]\lambda = \dot{\phi}\dot{\delta}. \tag{42}$$

In these equations, $\delta = \delta\rho/\rho$ is the density contrast, $\lambda = \delta\phi$, the parameter k is the wavenumber resulting from the Fourier decomposition of the perturbed quantities, and $\Omega_m = \Omega_{m0}/a^3$ is the density parameter for the matter component, Ω_{m0} being its value today. This density parameter contains two terms, the baryonic component and the dark matter component $\Omega_{m0} = \Omega_{b0} + \Omega_{dm0}$. Equations (41,42) refer to the Fourier transform of the fundamental quantities, that is, we should more properly write δ_k and λ_k.

In order to carry out the comparison with observations, it is more convenient to re-express equations (41,42) using the scale factor as dynamical variable. Moreover, we divide both equations by H_0^2, the Hubble parameter today. The final (dimensionless) equations are the following:

$$\delta'' + \left(\frac{2}{a} + \frac{f'}{f}\right)\delta' - \frac{3}{2}\frac{\Omega_m}{f^2}\delta = 2\frac{\dot{\phi}}{f}\lambda' - \frac{V_{\phi}}{f^2}\lambda, \tag{43}$$

$$\lambda'' + \left(\frac{3}{a} + \frac{f'}{f}\right)\lambda' + \left[\left(\frac{kl_0}{af}\right)^2 + \frac{V_{\phi\phi}}{f^2}\right]\lambda = \frac{\dot{\phi}}{f}\delta', \tag{44}$$

where the primes mean derivative with respect to a and $l_0 = 3.000h^{-1}\,Mpc$ is the Hubble radius. Moreover, the following definitions were used:

$$f(a) = \sqrt{\frac{\Omega_{m0}}{a} + \Omega_c(a)a^2}, \tag{45}$$

$$\dot{\phi}(a) = \sqrt{3\Omega_{c0}}\sqrt{g(a)^{1/(1+\alpha)} - \bar{A}g(a)^{-\alpha/(1+\alpha)}}, \tag{46}$$

$$V(a) = \frac{3}{2}\Omega_{c0}\left(g(a)^{1/(1+\alpha)} + \bar{A}g(a)^{-\alpha/(1+\alpha)}\right), \tag{47}$$

$$V_\phi(a) = \frac{f(a)}{\dot{\phi}}V'(a), \tag{48}$$

$$V_{\phi\phi}(a) = \frac{f(a)}{\dot{\phi}}V'_\phi(a), \tag{49}$$

$$\Omega_c(a) = \Omega_{c0}g(a)^{1/(1+\alpha)}. \tag{50}$$

In these expressions, Ω_{c0} is the density parameter for the generalized Chaplygin gas model, which obeys the flat condition $\Omega_{c0} + \Omega_{m0} = 1$ and $g(a)$ is given by (31).

Now, we compare the model with the power spectrum observational data from the 2dFGRS compilation in the range that corresponds to the linear regime, that is $0.01\,Mpc^{-1} < kh^{-1} < 0.185\,Mpc^{-1}$. This compilation mounts to 39 data. In the numerical computation, one important aspect is how to introduce the initial conditions. We use the BBKS transfer function [18], which gives the spectrum today for the ΛCDM model, integrating it back to the redshift $z = 1000$, where the initial condition are fixed. The general procedure is described in reference [19]. In comparison with this reference, there is an important modification. When $\alpha < -1$, the general behaviour is the dominance of an accelerated phase in the past, approaching a dust dominated universe in recent times. This scenario may bring problems concerning the formation of sctruture (to which extent it will be verified in what follow), but may be interesting to implement the ideia that the acceleration of the universe is a transient phase. In fact, in reference [20], it has been pointed out that the acceleration of the universe is slowing down. The important point is that, when $\alpha \lesssim -3$, the resulting scenario is very similar to the ΛCDM model until very recent times: for $\alpha \sim -3$ it is found $\dot{\phi} \sim 0$ and $V(\phi) =$ constant until $z \sim 20$. The general behaviour of $\dot{\phi}$ in terms of z and α is illustrated, for some specific cases, in figure (1). For $\alpha > -1$ this general behaviour is inverted. The fact that for α negative enough the model

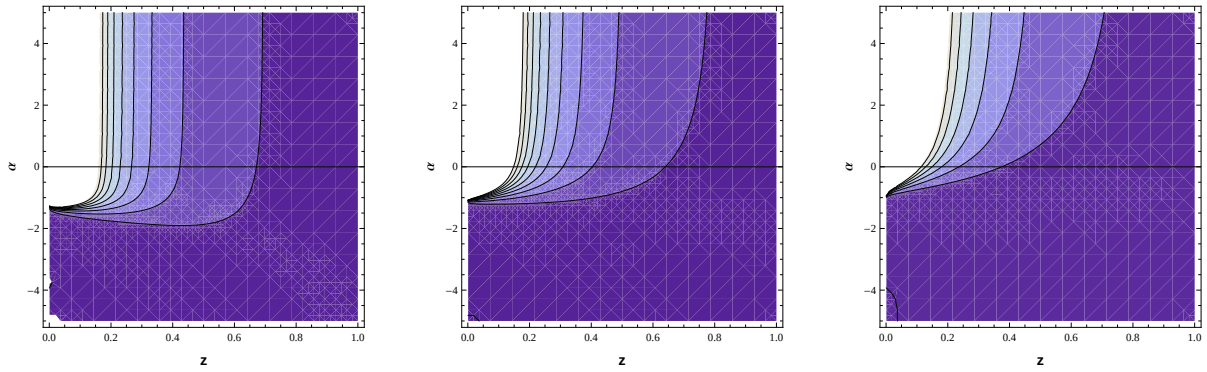

FIG. 1: Behaviour of $\dot{\phi}$ as function of α and z, fixing $\Omega_{m0} = 0.3$ for $\bar{A} = 0.1$ (left), 0.5 (center) and 0.9 (right). The darker colours indicate an almost zero value for $\dot{\phi}$.

is essentially ΛCDM until very recently does not allow to imposed the initial conditions using the transfer function with $\Omega_{m0} \sim 0.3$ and $\Omega_{\Lambda 0} = 0.7$ as it has been done in [19]. For $\alpha \lesssim -3$ the initial conditions must be imposed, due to computational reasons, about $z = 20$. Because of that, we must take into account the fact that the transfer function depends explicitly on the mass parameters.

The fundamental quantity to be evaluated is the matter power spectrum

$$P_k = \delta_k^2, \tag{51}$$

which is the Fourier transform of the two-points correlation function of matter distribution in the universe. We perform a bayesian statistic analysis, using first the χ^2 function

$$\chi^2 = \sum_{i=1}^{n} \frac{(P_{k_i}^o - P_{k_i}^t)^2}{\sigma_i^2}, \tag{52}$$

where $P_{k_i}^o$ is the i^{th} power spectrum observational data, with σ_i^2 observational error bar, $P_{k_i}^t$ its corresponding theoretical prediction. From this quantitity, we construct the Probability Distribution Function (PDF),

$$P = Ae^{-\chi^2/2}, \tag{53}$$

where A is a normalization constant. The PDF depends in general, for the GCG model, of 5 parameters: $\bar{A}$, α, Ω_{dm0} Ω_{c0} and Ω_{k0}, where the last quantity is associated with the curvature of the spatial section. The power spectrum is expressed as function of h, reducing the number of parameters to four. Imposing the flat condition $\Omega_{k0} = 0$, implies only 3 free parameters. We will perform a two-dimensional computation, fixing $\bar{A}$. All computations will be made considering three values of this quantity: $\bar{A} = 0.1, 0.5$ and 0.9. This will allow us to evaluate the influence of this parameter in the final results. We will plot the two dimensional PDF as well as the corresponding one dimensional PDF, by marginalizing (integrating) over the one of the variables.

The results indicate a very general pattern. Leaving α free, we remark the appearance of the two plateau in the PDF: one for $\alpha \lesssim -2.5$, and the other for $\alpha \gtrsim 1$. The plateau corresponding to the positive values of α is higher than the plateau corresponding to negative values. Hence, the model predicts, in some sense, that α must be positive. From figures (2,3,4) it is clear that the PDF is concentrated in the region of positive values for α and values for Ω_{dm0} in the range $0.2 < \Omega_{dm0} < 0.3$. These regions are displaced for larger positive values of α as $\bar{A}$ increases. There is another region with smaller probabilities for α negative - see figures (2,3,4) - which is almost not affected by changing $\bar{A}$. These behaviours are confirmed by considering the one dimensional PDF for α displayed in figure (3). Remark that there is a peak near $\alpha = -1$ which corresponds to a linear, constant, relation between pressure and density. We atribute this to effects corresponding to the numerical computation near the singular point - however, even increasing strongly the precision of the computation (implying increasing in the computational time), this peak does not disappear.

For the dark matter density parameter Ω_{dm0}, it is peaked quite generally around $\Omega_{dm0} = 0.23$. This is a result very similar to the ΛCDM model, and all framework is very close to the quintessence model (whose precise prediction depends on the choice of the potential for the scalar field). The parameter estimations at, for example, 1σ, 2σ, etc. for the parameter α becomes very doubtfull due to the existence of the two plateaus. It could be done for the parameter Ω_{dm0} due to its almost gaussian probability distribution, but even a visual analysis of figures (4) shows that they change very little with the increasing

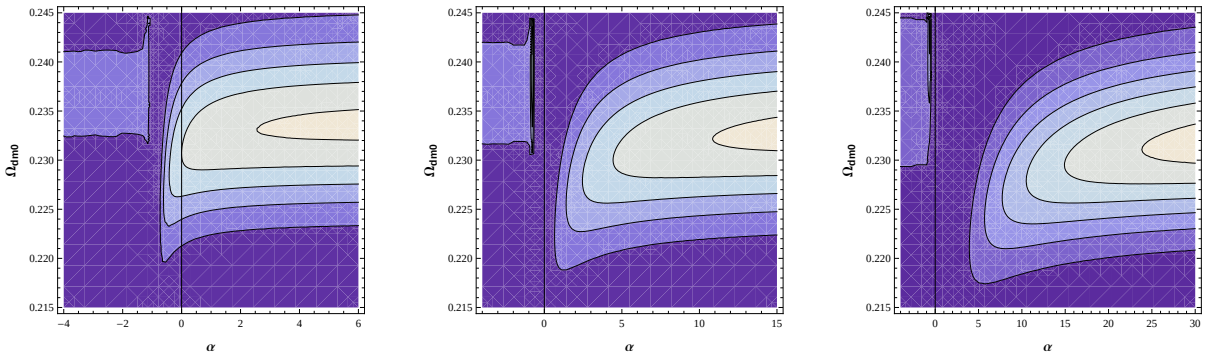

FIG. 2: Two dimensional PDF for the parameters Ω_{dm0} and α for $\bar{A} = 0.1$ (left), 0.5 (center) and 0.9 right.

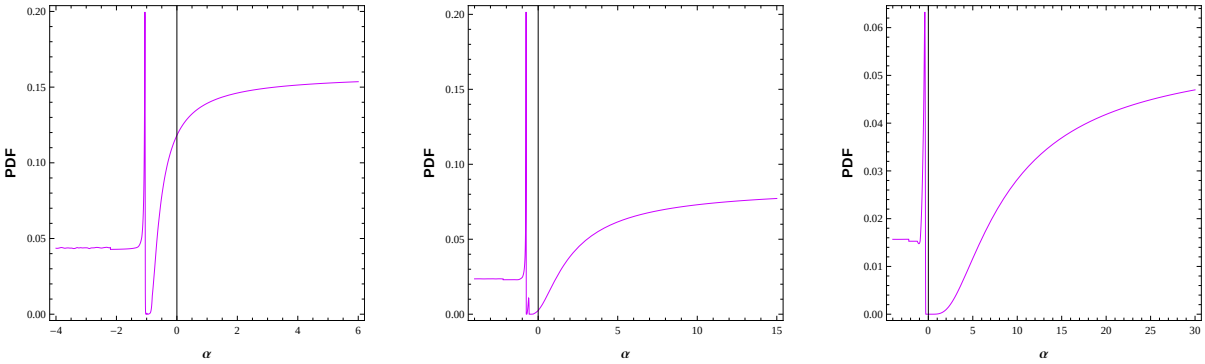

FIG. 3: One dimensional PDF for the parameter α for $\bar{A} = 0.1$ (left), 0.5 (center) and 0.9 right..

value of $\bar{A}$, remaining always peaked around 0.23.

It can be expected that the results may change by imposing some prior. One possibility is to restrict $\alpha > -1$. This restriction does not change the results, which are displayed in figure (5). Again, the maximum of probability for Ω_{dm0} is sharply peaked around 0.23, while there is a plateau for the PDF of α which, in this case, by fixing $\bar{A} = 0.5$, begins at $\alpha \sim 8$. However, some interesting effects appear if we fix, from the beginning, the

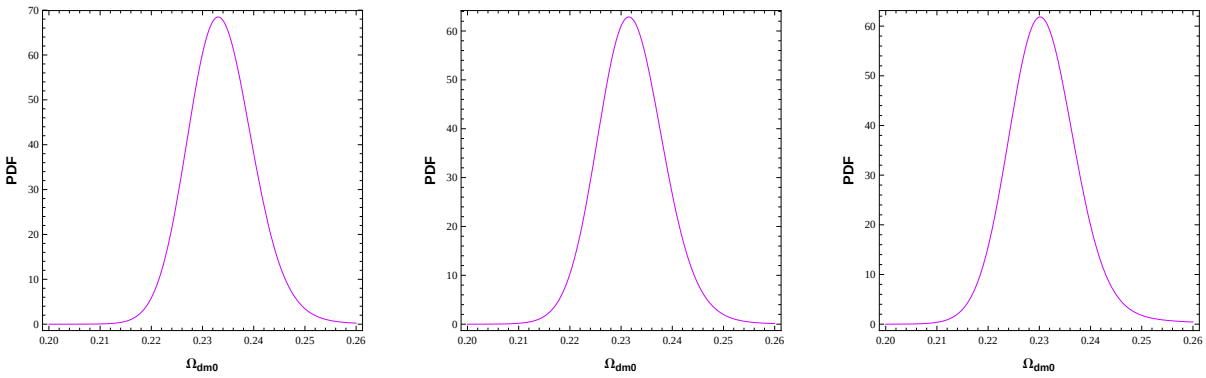

FIG. 4: One dimensional PDF for the parameter Ω_{dm0} for $\bar{A} = 0.1$ (left), 0.5 (center) and 0.9 right.

dark matter component equal to zero. This mounts to impose the unification scenario where the dark matter and dark energy are both represented by the Chaplygin gas model. In this case, two free parameters are considered: $\bar{A}$ and α. In figure (6) the results are displayed. The main feature to be remarked is that, now the maximum for PDF occurs for negative α. There are strong oscillations near $\alpha = -1$. In this case, the minimum for χ^2 may depend on the precision of the numerical evaluation. It can vary from, for example, $\chi^2 \sim 0.30$ for $\alpha \sim -0.85$, to $\chi^2 = 0.34$ for $\alpha = -0.88$ (using SN Ia, Gold sample, the favored value is $\alpha = -0.10$[11]). When the unification scenario is not imposed from the begining (the previous cases), it is found typically $\chi^2_{min} = 0.30$, in a more stable way. For a comparison, for the ΛCDM, we have $\chi^2_{min} \sim 0.38$, but with just one free parameter when the spatial section is flat. If the Akaike Information Criteria, AIC, is used, which allows to compare models with different number of free parameters ($AIC = 2 \times N + \chi^2_{total}$, where N is the number of free parameters), the ΛCDM model remains the best one, but the difference is very small: $AIC \sim 18$ for the scalar GCG model with three free parameters, $AIC \sim 17 - 18$, for the unified scalar GCG model with two free parameters, while $AIC \sim 17$ for the ΛCDM model.

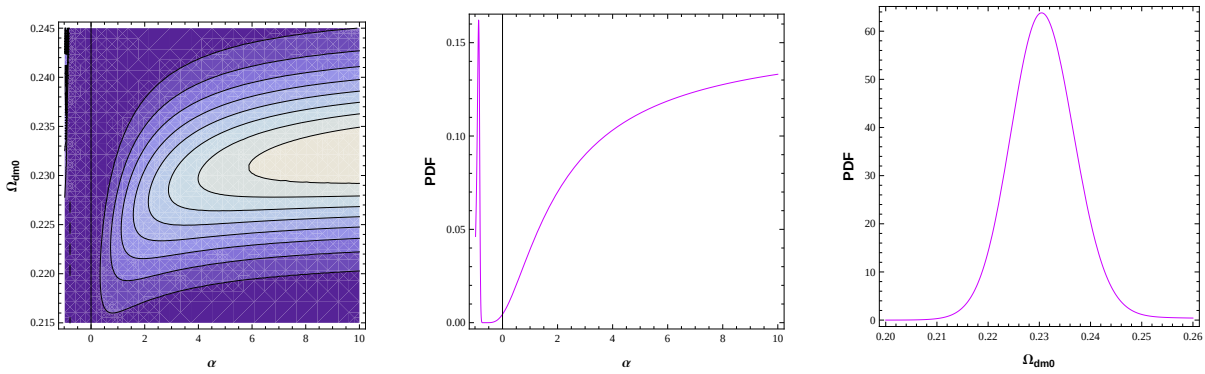

FIG. 5: Two and one dimensional PDFs restricting $\alpha > -1$ and fixing $\bar{A} = 0.5$.

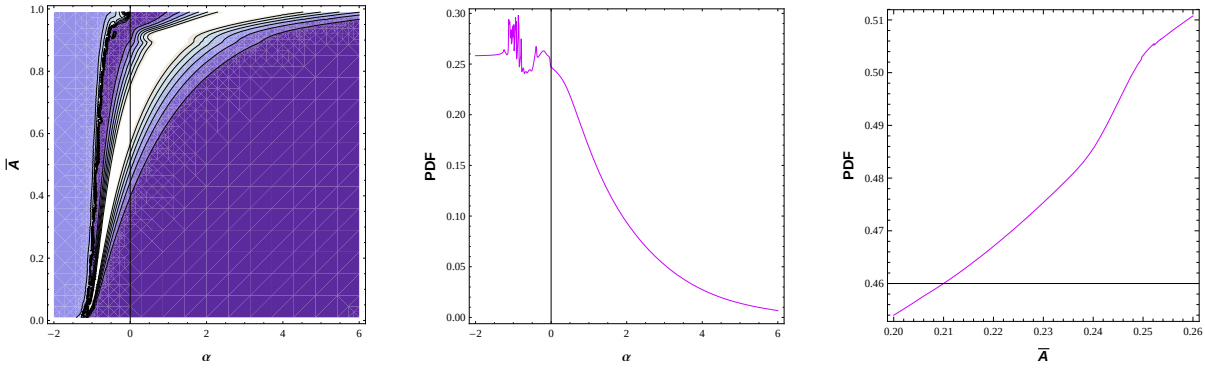

FIG. 6: Two and one dimensional PDFs restricting $\Omega_{dm0} = 0$.

VI. CONCLUSIONS

We have investigate here the possibility that the Generalized Chaplygin Gas (GCG) model may be represented by a self-interacting scalar field, instead of using the fluid representation or the Dirac-Born-Infeld (DBI) action for a tachyonic fluid. The main reason for this investigation is that both the fluid or DBI representations forbid to extend the analysis of the CGG model to negative values of α at perturbative level, due to a negative squared sound velocity, which drives strong instabilities. This represents a strong restriction, mainly when it is took into account that some background observational tests, like SN Ia, favor negative values of α.

We have shown initially that, for the GCG model, the fluid representation is equivalent to the tachyonic representation of the generalized DBI action, at background and

perturbative levels, extending the results reference [17]. Hence, in order to consider the possibility of having negative values for α in a perturbative analysis, we must use another framework, which we have choosen that one represented by a self-interacting scalar field. In this case, negative values for α does not lead to any problem connected with the sign of the (squared) sound velocity. When baryons are presented, there is no closed form for the potential representing the GCG, but an implicit expression, using the scale factor as variable, can be obtained.

We have made a statistic analysis using the perturbative expressions for the self-interacting scalar field model for the GCG, computing the matter power spectrum for the matter component, and confronting it with the 2dFGRS observational data. In principle, we allow the presence of dark matter besides baryons and the scalar field. The constraints obtained indicate that a kind of quintessence scenario emerges, with $\Omega_{dm0} \sim 0.23$ (like in the ΛCDM model). High positive values of α are favored. The best fitting configuration implies typically $\chi^2_{min} \sim 0.30$, better than in the case of the ΛCDM model, for which $\chi^2_{min} \sim 0.38$.

An interesting scenario emerges when the unification scenario is imposed from the beginning, fixing $\Omega_{dm0} = 0$. The best fitting is $\chi^2_{min} \gtrsim 0.30$, still smaller than in the ΛCDM case, but now for α negative. This is qualitatively in agreement with the SN Ia analysis. Perhaps this may indicate a new concordance model, different from the ΛCDM. However, a more deep perturbative analysis must be performed, mainly using the Integrated Sachs-Wolfe effect (a very delicate test for the unified models [21]), or even the full anisotropy spectrum of CMB. We hope to present this analysis in the future.

Acknowledgement We thank CNPq (Brazil) for partial financial support.

---

[1] E. Komatsu et al., *Seven-year Wilkinson microwave anisotropy probe (WMAP) observations: cosmological interpretation*, arXiv:1001.4538.

[2] R.R. Caldwell and M. Kamionkowski, Ann. Rev. Nucl. Part. Sci. **59**, 397(2009).

[3] G. Bertone, D. Hooper and J. Silk, Phys. Rep. **405**, 279(2005).

[4] T. Padmanabhan, Phys. Rep. **380**, 235(2003).

[5] J. Martin, Mod. Phys. Lett. **A23**, 1252(2008).

[6] A.Y. Kamenshchik, U. Moschella and V. Pasquier, Phys. Lett. **B511**, 265(2001).

[7] M.C. Bento, O. Bertolami and A.A. Sen, Phys. Rev. **D66**, 043507 (2002).

[8] N. Bilic, G.B. Tupper and R.D. Viollier, Phys. Lett. **B535**, 17(2002).

[9] J.C. Fabris, S.V.B. Gonçalves and P.E. de Souza, Gen. Rel. Grav. **34**, 53(2002).

[10] R. Jackiw, *A particle field theorist's lectures on supersymmetric, non abelian fluid mechanics and d-branes*, physics/0010042.

[11] R. Colistete Jr, J. C. Fabris, S.V.B. Gonçalves and P.E. de Souza, Int. J. Mod. Phys. D13, 669(2004); R. Colistete Jr., J. C. Fabris and S.V.B. Gonçalves, Int. J. Mod. Phys. D14, 775(2005); R. Colistete Jr. and J. C. Fabris, Class. Quant. Grav. 22, 2813(2005).

[12] T. Barreiro, O. Bertolami and P. Torres, Phys. Rev. **D78**, 043530(2008).

[13] L. Amendola, F. Finelli, C. Burigana and D. Carturan, JCAP **0307**, 005(2003).

[14] O. Piattella, JCAP **1003**, 012(2010).

[15] V. Gorini, A. Y. Kamenshchik, U. Moschella, O. F. Piattella and A. A. Starobinsky, JCAP **0802**, 016(2008).

[16] J.C. Fabris, S.V.B. Gonçalves, H.E.S. Velten and W. Zimdahl, Phys. Rev. D78, 103523 (2008). J.C. Fabris, H.E.S. Velten and W. Zimdahl, Phys. Rev. D81, 087303(2010).

[17] C.E.M. Batista, J.C. Fabris and M. Morita, Gen. Rel. Grav. **42**, 839(2010).

[18] N. Sugiyama, Astrophys. J.Suppl. **100**, 281(1995); J.M. Bardeen, J.R. Bond, N. Kaiser and A.S. Szalay, Astrophys. J. **304**, 15 (1986).

[19] J.C. Fabris, J. Solà and I.L. Shapiro, JCAP **0702**,016(2007).

[20] A. Shafieloo, V. Sahni and A.A. Starobinsky, Phys. Rev. **D80**, 101301(2009).

[21] B. Li and J.D. Barrow, Phys. Rev.**D79**,103521(2009).